

**Activity measurements of the radionuclides  $^{99m}\text{Tc}$ ,  $^{18}\text{F}$  and  $^{64}\text{Cu}$  for the POLATOM,  
Poland, in the ongoing comparisons BIPM.RI(II)-K4 series  
and KCRV update in the corresponding BIPM.RI(II)-K1 comparison**

C. Michotte<sup>1</sup>, T. Dziel<sup>2</sup>, A. Listkowska<sup>2</sup>, T. Ziemek<sup>2</sup>, Z. Tymiński<sup>2</sup>, I. Da Silva<sup>3</sup>

<sup>1</sup> Bureau International des Poids et Mesures (BIPM), 92 310 Sèvres

<sup>2</sup> National Centre for Nuclear Research, Radioisotope Centre (POLATOM), 05-400 Otwock

<sup>3</sup> CNRS/CEMHTI, Orléans, France

## Abstract

In 2016, comparisons of activity measurements of  $^{99m}\text{Tc}$ ,  $^{18}\text{F}$  and  $^{64}\text{Cu}$  using the Transfer Instrument of the International Reference System (SIRTI) took place at the National Centre for Nuclear Research, Radioisotope Centre (POLATOM, Poland). Ampoules containing about 33 kBq of  $^{99m}\text{Tc}$ , 28 kBq of  $^{18}\text{F}$  and 110 kBq of  $^{64}\text{Cu}$  solutions were measured in the SIRTI for about 3, 5 and 1.5 half-lives, respectively. The POLATOM standardized the activity in the ampoules by  $4\pi(\text{LS})\beta\text{-}\gamma$  coincidence measurements. The comparisons, identifiers BIPM.RI(II)-K4.Tc-99m, BIPM.RI(II)-K4.F-18 and BIPM.RI(II)-K4.Cu-64, are linked to the corresponding BIPM.RI(II)-K1.Tc-99m, BIPM.RI(II)-K1.F-18 and BIPM.RI(II)-K1.Cu-64 comparisons. The BIPM.RI(II)-K1  $^{99m}\text{Tc}$  and  $^{18}\text{F}$  key comparison reference values have been updated to include the latest BIPM.RI(II)-K4 linked results and degrees of equivalence for both comparison series have been evaluated.

## 1. Introduction

Radionuclides are essential for nuclear medicine for which radionuclides with half-life often much less than one day are used, particularly for imaging. The use of nuclear medicine is increasing with the accessibility of these radionuclides which are consequently of great interest to the National Metrology Institutes (NMIs) in terms of standardization and SI traceability. However, sending ampoules of short-lived radioactive material to the Bureau International des Poids et Mesures (BIPM) for measurement in the International Reference System (SIR) [1] is only practicable for the NMIs that are based in Europe and near to the BIPM. Consequently, to extend the utility of the SIR and enable other NMIs to participate, a transfer instrument (SIRTI) has been developed at the BIPM with the support of the Consultative Committee for Ionizing Radiation CCRI(II) Transfer Instrument Working Group [2].

The BIPM ongoing K4 comparisons of activity measurements of  $^{99m}\text{Tc}$  (half-life  $T_{1/2} = 6.0067\text{ h}$ ;  $u = 0.001\text{ h}$  [3])<sup>1</sup>,  $^{18}\text{F}$  (half-life  $T_{1/2} = 1.8288(3)\text{ h}$  [3]) and  $^{64}\text{Cu}$  (half-life of

---

<sup>1</sup> Hereafter, the last digits of the standard uncertainties are given in parenthesis.

12.7004(20) h [4]) are based on the SIRTI, a well-type NaI(Tl) crystal calibrated against the SIR, which is moved to each participating laboratory. The stability of the system is monitored using a  $^{94}\text{Nb}$  reference source (half-life of 20 300(1 600) years [5]) from the Joint Research Centre of the European Commission (JRC, Geel), which also contains the  $^{93\text{m}}\text{Nb}$  isotope. The  $^{99\text{m}}\text{Tc}$ ,  $^{18}\text{F}$  or  $^{64}\text{Cu}$  count rate above a low-energy threshold, defined by the  $^{93\text{m}}\text{Nb}$  x-ray peak at 16.6 keV, is measured relative to the  $^{94}\text{Nb}$  count rate above the same threshold. Once the threshold is set, a brass liner is placed in the well to suppress the  $^{93\text{m}}\text{Nb}$  contribution to the  $^{94}\text{Nb}$  stability measurements. It should be noted that the uncertainty associated with the  $^{94}\text{Nb}$  decay correction is negligible. The  $^{99\text{m}}\text{Tc}$  SIR ampoule is placed in the detector well in a brass liner; for the  $^{18}\text{F}$  and  $^{64}\text{Cu}$  SIR ampoules, a PVC (polyvinyl chloride) liner is used instead to stop the  $\beta^+$  particles while minimizing the production of bremsstrahlung. No extrapolation to zero energy is carried out as all the measurements are made with the same threshold setting. The live-time technique using the MTR2 module from the Laboratoire National d'Essais – Laboratoire National Henri Becquerel, France (LNE-LNHB) [6] is used to correct for dead-time losses, taking into account the width of the oscillator pulses. The standard uncertainty associated with the live-time correction, due to the effect of the finite frequency of the oscillator, is negligible.

Similarly to the SIR, a SIRTI equivalent activity,  $A_E$ , is deduced from the  $^{99\text{m}}\text{Tc}$ ,  $^{18}\text{F}$  or  $^{64}\text{Cu}$  and the  $^{94}\text{Nb}$  counting results and the  $^{99\text{m}}\text{Tc}$ ,  $^{18}\text{F}$  or  $^{64}\text{Cu}$  activity measured by the NMI.  $A_E$  is inversely proportional to the detection efficiency, i.e..  $A_E$  is the activity of the source measured by the participant divided by the  $^{99\text{m}}\text{Tc}$ ,  $^{18}\text{F}$  or  $^{64}\text{Cu}$  count rate in the SIRTI relative to the  $^{94}\text{Nb}$  count rate. The possible presence of impurity in the solution should be accounted for using  $\gamma$ -ray spectrometry measurements carried out by the NMI.

The current K4 comparisons are linked to the corresponding BIPM.RI(II)-K1 comparisons through the calibration of the SIRTI against the SIR at the BIPM and, consequently, the degrees of equivalence with the K1 key comparison reference value (KCRV) can be evaluated. The K4  $^{99\text{m}}\text{Tc}$  and  $^{18}\text{F}$  comparison results based on primary measurements carried out by the NMI, or ionization chamber measurements traceable to primary  $^{99\text{m}}\text{Tc}$  and  $^{18}\text{F}$  measurements are eligible for inclusion in the KCRV, with some restrictions.

The protocol [7] and previous comparison results for the BIPM.RI(II)-K4 comparisons are available in the key comparison database of the CIPM (International Committee on Weights and Measures) Mutual Recognition Arrangement [8]. Publications concerning the details of the SIRTI and its calibration against the SIR can be found elsewhere [9, 10].

## 2. Participants

As detailed in the protocol, participation in the BIPM.RI(II)-K4 comparisons mainly concerns member states that are located geographically far from the BIPM and that have developed a primary measurement method for the radionuclide of concern. However, at the time of the comparison, the NMI may decide for convenience to use a secondary method, for example a calibrated ionization chamber. In this case, the traceability of the calibration needs to be clearly identified.

The present comparisons took place at the National Centre for Nuclear Research, Radioisotope Centre (POLATOM), Poland, in October 2016, which used the  $4\pi(\text{LS})\beta\text{-}\gamma$  coincidence method for the activity standardizations.

### 3. The SIRTI at the POLATOM

The reproducibility and stability of the SIRTI at the POLATOM were checked by measuring the count rate produced by the reference  $^{94}\text{Nb}$  source No. 1, the threshold position (defined by the  $^{93\text{m}}\text{Nb}$  x-ray peak), the background count rate, the frequency of the oscillator No. 1 for the live-time correction and the room temperature as shown in Figure 1a. The plots shown in the Figure represent the differences from the values indicated in the figure caption, using the appropriate units, as given, for each quantity measured.

The SIRTI background measured at the POLATOM was fluctuating in relation with manipulation of large activities of  $^{131}\text{I}$  and  $^{99}\text{Mo}/^{99\text{m}}\text{Tc}$  in the building, use of a reactor on the site and transport of radionuclide solutions to customers on the road close to the laboratory. Fig. 1b shows fluctuations and spikes observed in the background count rate. For this reason, it was decided to include in the comparison analysis only those measurements made at a count rate higher than  $4000\text{ s}^{-1}$ .

The SIRTI has been stable during the comparison as shown by the  $^{94}\text{Nb}$  measurement results in Figure 1a. The mean  $^{94}\text{Nb}$  No. 1 count rate, corrected for live-time, background, and decay, measured at the POLATOM, was  $8493.8(5)\text{ s}^{-1}$  and was used to normalize the  $^{99\text{m}}\text{Tc}$ ,  $^{18}\text{F}$  and  $^{64}\text{Cu}$  count rates. This mean value agrees within two combined standard uncertainties with the weighted mean of the  $^{94}\text{Nb}$  No. 1 count rate since the set-up of the system in March 2007,  $8492.71(22)\text{ s}^{-1}$ .

Finally, on the return of the SIRTI to the BIPM after the POLATOM comparison, the  $^{94}\text{Nb}$  count rate was checked giving a value of  $8494.6(18)\text{ s}^{-1}$  in agreement with the measurements carried out at the POLATOM. Background measurements were also repeated at the BIPM for about 120 h, giving a stable background value of  $82.28(7)\text{ s}^{-1}$  and no observable spike. This demonstrates that the fluctuations and spikes observed at the POLATOM were real and not due to some artefact of the SIRTI.

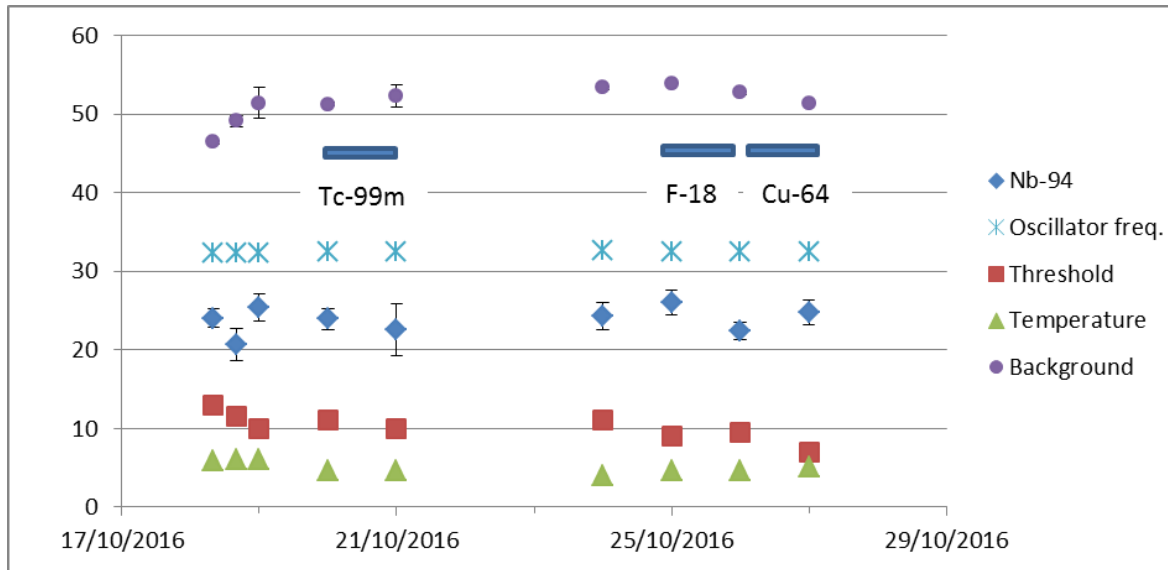


Figure 1a: Fluctuation of the SIRT I at the POLATOM. Diamonds:  $^{94}\text{Nb}$  No.1 count rate /  $\text{s}^{-1}$  above  $8470 \text{ s}^{-1}$ ; stars: frequency of the oscillator No.1 /  $\text{Hz}$  above  $999\,970 \text{ Hz}$ ; squares: threshold position / channel above 95 channels; triangles: room temperature /  $^{\circ}\text{C}$  above  $15 \text{ }^{\circ}\text{C}$ ; circles: background count rate /  $\text{s}^{-1}$  above  $60 \text{ s}^{-1}$ . Statistical uncertainty ( $k = 1$ ) for the Nb source, threshold position and background are shown (in some cases the uncertainties are not visible in the plot as they are hidden by the character printed for the data point).

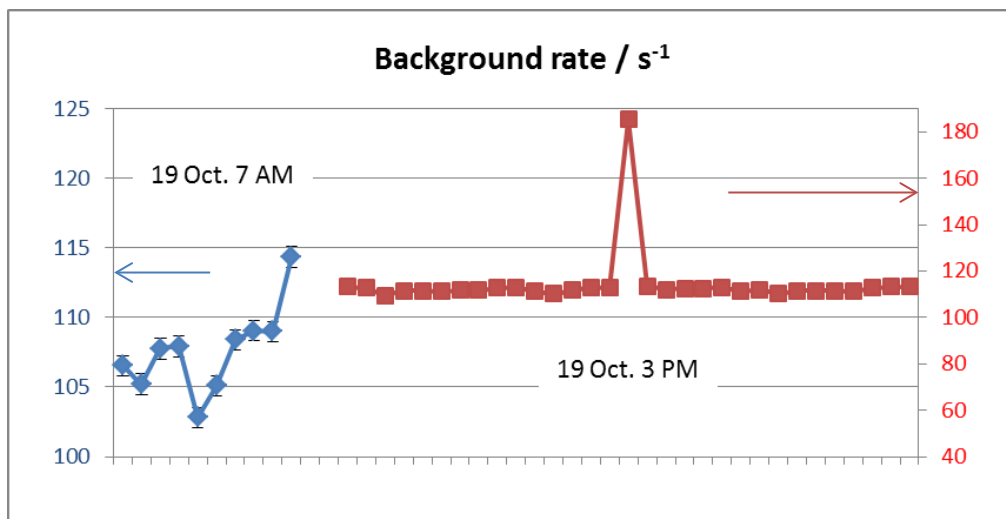


Figure 1b: examples of background fluctuations over time observed with the SIRT I at the POLATOM. In blue (10 measurements of 500 s) is an example of fluctuations probably related to manipulation of high activity sources in the building at the beginning of the production day; in red (32 measurements of 100 s) shows a spike due to the transport of high activity sources on the road next to the room where the SIRT I was installed.

#### 4. The $^{99m}\text{Tc}$ , $^{18}\text{F}$ and $^{64}\text{Cu}$ solutions standardized at the POLATOM

The  $^{99m}\text{Tc}$ ,  $^{18}\text{F}$  and  $^{64}\text{Cu}$  solutions measured in the SIRTI are described in Table 1, including any impurities, when present, as identified by the laboratory. Two SIR ampoules were prepared from each solution for measurement in the SIRTI. The density and volume of the solutions in the ampoules conformed to the K4 protocol requirements. Several small drops were present in the cylindrical part of the  $^{99m}\text{Tc}$  ampoules. During the measurement series one drop (diameter  $\sim 1$  mm) appeared in the neck of ampoule R2-1 and several drops of diameter  $< 0.5$  mm in the ampoule head. The ampoule was centrifuged. No significant effect on the SIRTI results could be observed. For the  $^{18}\text{F}$  and  $^{64}\text{Cu}$  ampoules, similar drops were observed but the effect on the results is expected to be even lower than that for  $^{99m}\text{Tc}$ .

Table 1: Characteristics of the solutions measured in the SIRTI

Radionuclide	Solvent / mol dm <sup>-3</sup>	Carrier / $\mu\text{g g}^{-1}$	Density at 20 °C / g cm <sup>-3</sup>	Ampoule number	Mass / g	Impurity*
$^{99m}\text{Tc}$	water	NaCl / 9000	1.0	BW/29/16/ R2-1	3.625 25	$^{99}\text{Mo}: 2.3(1) \times 10^{-4}$
				BW/29/16/ R2-2	3.631 03	
$^{18}\text{F}$	water	NaCl / 9000	1.0	BW/30/16/ R2-1	3.631 13	$^{48}\text{V}: 3.0(2) \times 10^{-9}$ $^{96}\text{Tc}: 2.1(1) \times 10^{-9}$
				BW/30/16/ R2-2	3.619 59	
$^{64}\text{Cu}$	HCl / 0.1	-	1.0	BW/31/16/ R2-1	3.607 07	$^{67}\text{Cu}: 9.5(2) \times 10^{-7}$ $^{186}\text{Re}: 2.8(1) \times 10^{-6}$ $^{76}\text{As}: 1.1(1) \times 10^{-6}$
				BW/31/16/ R2-2	3.604 30	

\* Ratio of the impurity activity to the main radionuclide activity at the reference date

The  $^{99m}\text{Tc}$ ,  $^{18}\text{F}$  and  $^{64}\text{Cu}$  master solutions were diluted and the 1<sup>st</sup> diluted solutions were obtained (dilution factor  $R_1$ ). Each of the 1<sup>st</sup> diluted solutions was used for preparation of a set of twelve sources in 10 mL Ultima Gold liquid scintillator (LS-sources). High performance PerkinElmer glass vials of 20 mL were used. Standardization was performed at POLATOM by the  $4\pi(\text{LS})$ - $\gamma$  coincidence primary method. A window in the gamma-channel of the  $4\pi(\text{LS})$ - $\gamma$  coincidence counter was set at the  $\gamma$  peak of each radionuclide: 511.0 keV for  $^{18}\text{F}$ , 511.0 keV for  $^{64}\text{Cu}$  and 140.5 keV for  $^{99m}\text{Tc}$ . The counting efficiency in the beta-channel was changed by varying the voltage at the photomultiplier anodes. The activity concentration of the  $^{99m}\text{Tc}$ ,  $^{18}\text{F}$  and  $^{64}\text{Cu}$  solutions was determined using the linear extrapolation method.

The 1<sup>st</sup> diluted solutions were then diluted to obtain the 2<sup>nd</sup> diluted solutions (dilution factor  $R_2$ ). Each of the 2<sup>nd</sup> diluted solutions was used for preparation of a set of two ampoules for measurement in the SIRTI. The scheme of all dilutions is shown in Fig. 2.

The  $^{99m}\text{Tc}$ ,  $^{18}\text{F}$  and  $^{64}\text{Cu}$  activities in the SIRTI ampoules were deduced from the measurements of the LS-sources. The measurement results are summarized in Tables 2 and 3.

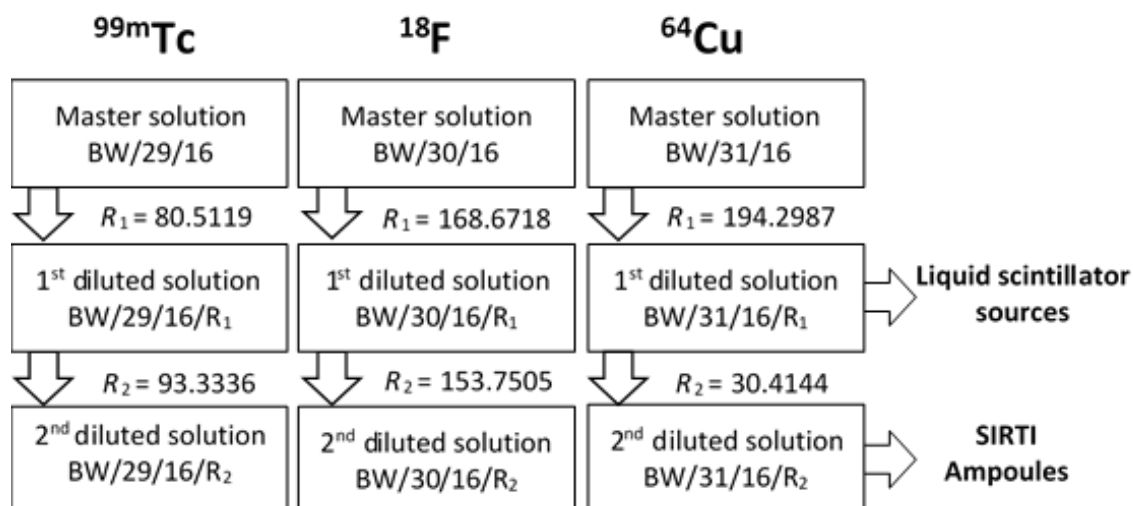


Figure 2: Scheme of dilution of the  $^{99m}\text{Tc}$ ,  $^{18}\text{F}$  and  $^{64}\text{Cu}$  master solutions with dilution factors  $R_1$  and  $R_2$

Table 2: The  $^{99m}\text{Tc}$ ,  $^{18}\text{F}$  and  $^{64}\text{Cu}$  standardizations by the POLATOM

Radionuclide	Measurement method ACRONYM*	Activity conc. / $\text{kBq g}^{-1}$	Standard uncert. / $\text{kBq g}^{-1}$	Reference date YYYY-MM-DD	Half-life used by the NMI / h
$^{99m}\text{Tc}$	$4\pi(\text{LS})\text{ce-}\gamma$ coincidence counting 4P-LS-CE-NA-GR-CO	8.927	0.064	2016-10-20 10:00 UTC	6.0067(10)
$^{18}\text{F}$	$4\pi(\text{LS})\beta^+-\gamma$ coincidence counting 4P-LS-PO-NA-GR-CO	7.738	0.043	2016-10-25 10:00 UTC	1.828 90(23)
$^{64}\text{Cu}$	$4\pi(\text{LS})\beta^+-\gamma$ coincidence counting 4P-LS-MX-NA-GR-CO	30.22	0.17	2016-10-26 10:00 UTC	12.7004(20)

\* See appendix 1

Table 3: The POLATOM uncertainty budgets for the activity measurement of the  $^{99m}\text{Tc}$ ,  $^{18}\text{F}$  and  $^{64}\text{Cu}$  ampoules

Uncertainty contributions due to	Evaluation method	Relative standard uncertainty $\times 10^4$		
		$^{99m}\text{Tc}$	$^{18}\text{F}$	$^{64}\text{Cu}$
Counting statistics	A	31	5	6
Weighing	A	7	15	15
Dead-time	B	1	1	1
Resolving time	B	36	5	5
Background	B	1	1	1
Counting time	B	1	1	1
Input parameters and statistical model	B	10	10	10
Decay-scheme parameters	B	15	15	15
Decay correction	B	2	5	1
Extrapolation of efficiency curve	B	50	50	50
<b>Relative combined standard uncertainty</b>		72	56	59

## 5. The $^{99m}\text{Tc}$ , $^{18}\text{F}$ and $^{64}\text{Cu}$ measurements in the SIRTl at the POLATOM

The maximum live-time corrected count rate in the NaI(Tl) was  $19\,400\text{ s}^{-1}$ , which conforms to the limit of  $20\,000\text{ s}^{-1}$  set in the protocol [7]. In addition, a relative standard uncertainty of  $4 \times 10^{-4}$ ,  $3 \times 10^{-4}$  and  $3 \times 10^{-4}$  for  $^{99m}\text{Tc}$ ,  $^{18}\text{F}$  and  $^{64}\text{Cu}$  respectively, was added to take account of a possible drift in the SIRTl at high count rate [9]. The time of each SIRTl measurement was obtained from the synchronization of the SIRTl laptop with a local NTP time server.

In principle, the live-time correction should be modified to take into account the decaying count rate [11]. In the present experiments, the duration of the measurements made at high rate has been limited to 700 s, 400 s and 700 s for  $^{99m}\text{Tc}$ ,  $^{18}\text{F}$  and  $^{64}\text{Cu}$ , respectively, so that the relative effect of decay on the live-time correction is less than one part in  $10^4$ .

Two ampoules of each of the  $^{99m}\text{Tc}$ ,  $^{18}\text{F}$  and  $^{64}\text{Cu}$  solutions were measured alternatively for 3, 5 and 1.5 half-lives, respectively, and the results are shown in Figures 3a, 3b and 3c. Because of fluctuations in the background (see section 3 above), only part of the measurement results was used in the analysis as indicated on the graphs for  $^{99m}\text{Tc}$  and  $^{18}\text{F}$ .

The reduced chi-squared values evaluated for these series of measurements are 0.93, 1.34 and 0.92 for  $^{99m}\text{Tc}$ ,  $^{18}\text{F}$  and  $^{64}\text{Cu}$ , respectively. The absence of significant trend confirms the stability

and adequate live-time and impurity corrections of the SIRTl. For  $^{99m}\text{Tc}$ , the largest impurity correction in the SIRTl measurements (21 h after the reference date) amounts to 1.00245(8) while for  $^{18}\text{F}$  and  $^{64}\text{Cu}$ , the correction is negligible ( $< 3 \times 10^{-5}$ ).

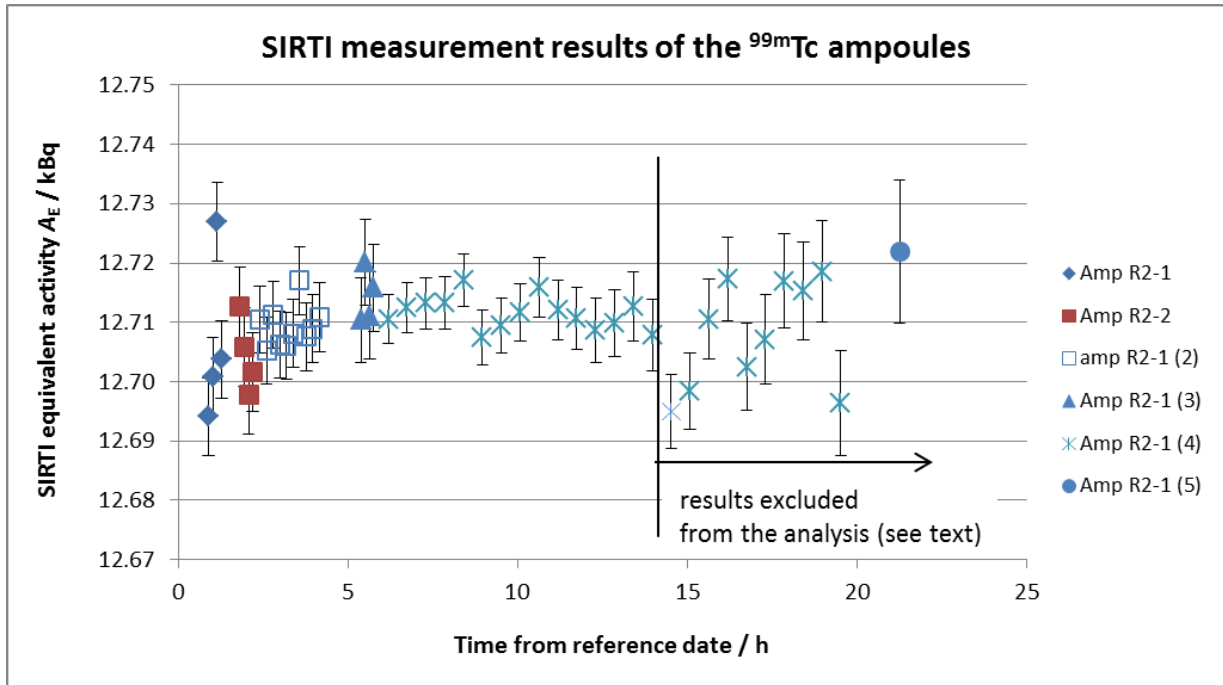


Figure 3a: The  $^{99m}\text{Tc}$  measurement results in the SIRTl at the POLATOM. The uncertainty of the  $^{99m}\text{Tc}$  activity concentration, which is constant over all the measurements, is not included in the uncertainty bars shown on the graph.

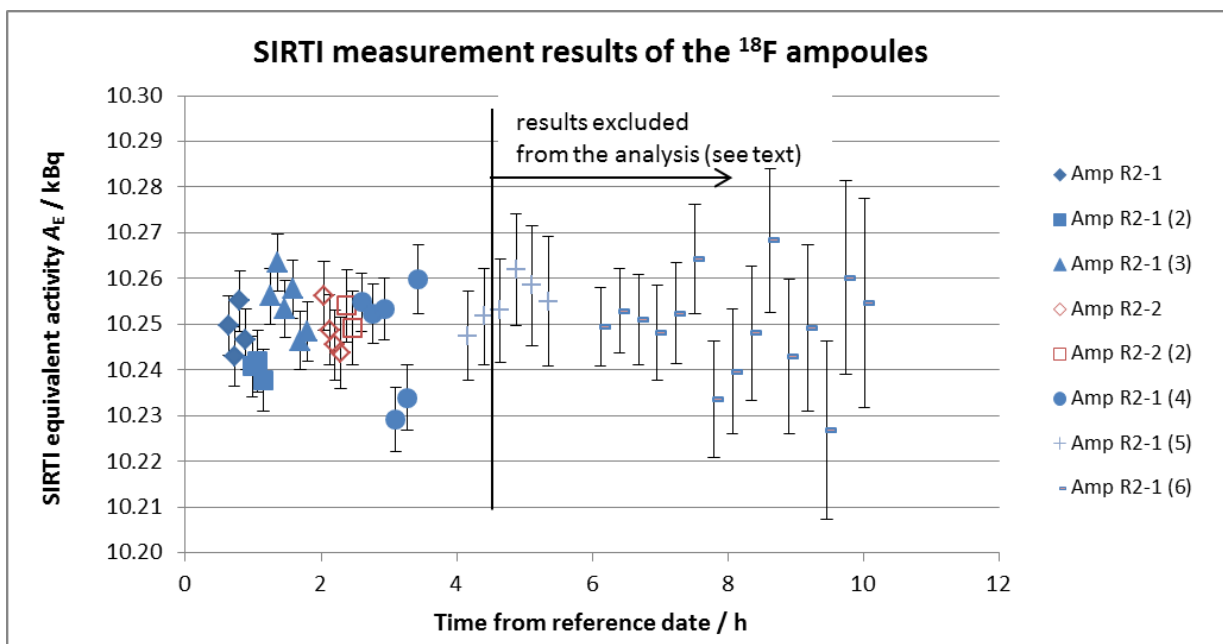


Figure 3b: As for Figure 3a, but for  $^{18}\text{F}$



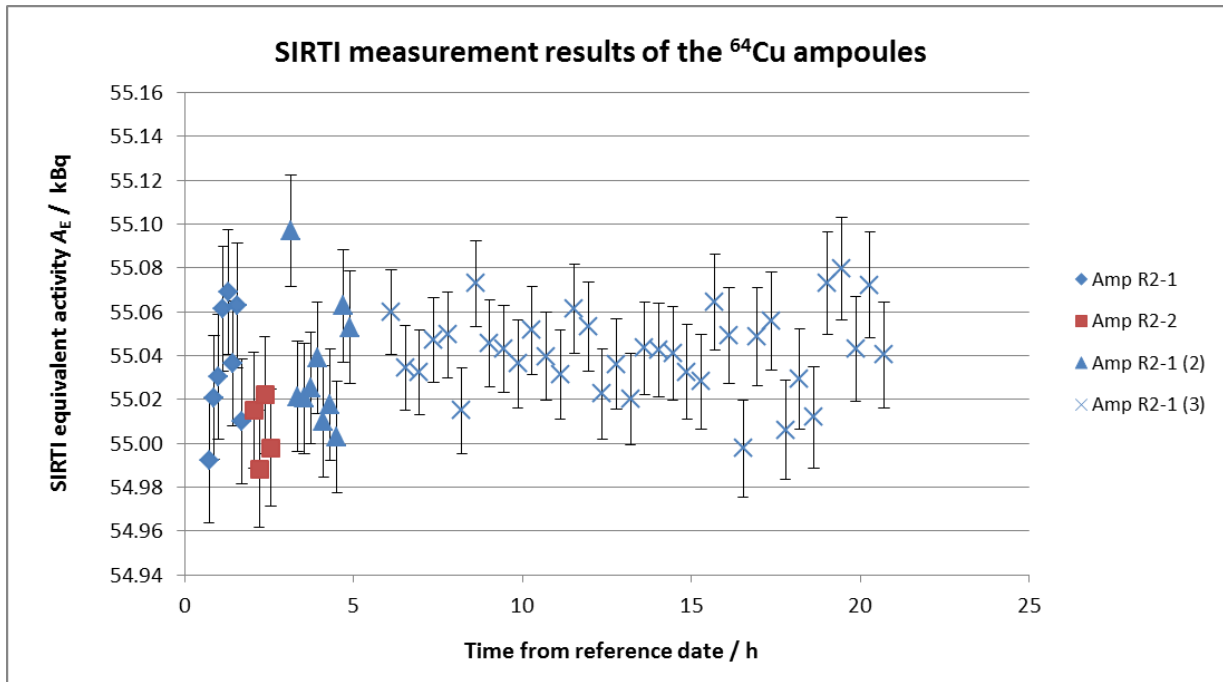


Figure 3c: As for Figure 3a, but for  $^{64}\text{Cu}$ . All measurements were used in the analysis.

The uncertainty budgets for the SIRTI measurements of the  $^{99\text{m}}\text{Tc}$ ,  $^{18}\text{F}$  and  $^{64}\text{Cu}$  ampoules are given in Table 4. In the SIRTI, the dominant part of the  $^{64}\text{Cu}$  detection efficiency is defined by its beta plus decay. In this sense it is similar to  $^{18}\text{F}$ , and the Monte-Carlo simulations carried out for  $^{18}\text{F}$  were also used for the  $^{64}\text{Cu}$  uncertainty evaluation. Further details are given in reference [9].

Table 4: Uncertainty budgets for the SIRTI measurement of the  $^{99m}\text{Tc}$ ,  $^{18}\text{F}$  and  $^{64}\text{Cu}$  ampoules

Uncertainty contributions due to	Comments	Evaluation method	Relative standard uncertainty $\times 10^4$		
			$^{99m}\text{Tc}$	$^{18}\text{F}$	$^{64}\text{Cu}$
Radionuclide counting including live-time, background, decay correction and threshold setting		A	1.8 <sup>§</sup>	3.3 <sup>§§</sup>	1.6 <sup>§§§</sup>
Mean $^{94}\text{Nb}$ count rate over the comparison at POLATOM	Standard uncertainty of the weighted mean of 9 series of 10 measurements	A	0.6	0.6	0.6
Long-term stability of the SIRTI	Weighted standard deviation of 90 series of 10 measurements	A	0.3	0.3	0.3
Effect of decay on the live-time correction	Maximum measurement duration evaluated from [12]	B	< 1	< 1	< 1
SIRTI drift at high count rate	Mean possible drift over the radionuclide series of measurements at the POLATOM	B	4	3	3
Ampoule dimensions	From the JRC report [13] and sensitivity coefficients from Monte-Carlo simulations	B	8	2.2	2.2
Ampoule filling height	Solution volume is 3.6(1) cm <sup>3</sup> ; sensitivity coefficients from Monte-Carlo simulations	B	2.8	2.3	2.3
Solution density	Between 1 g/cm <sup>3</sup> and 1.01 g/cm <sup>3</sup> as requested in the protocol; sensitivity coefficients from Monte-Carlo simulations	B	0.8	0.7	0.7
Drops on the ampoule walls	From Monte-Carlo simulation	B	2	2	2
<b>Relative combined standard uncertainty</b>			9.8	6.0	5.2

§ Standard uncertainty of the weighted mean of 37 measurements, taking into account the correlation due to the  $^{99m}\text{Tc}$  half-life

§§ Standard uncertainty of the weighted mean of 27 measurements, taking into account the correlation due to the  $^{18}\text{F}$  half-life

§§§ Standard uncertainty of the weighted mean of 58 measurements, taking into account the correlation due to the  $^{18}\text{F}$  half-life

## 6. Comparison results

The weighted mean and uncertainty of a selection of the measured  $A_E$  values is calculated taking into account correlations. The standard uncertainty  $u(A_E)$  is obtained by adding in quadrature the SIRTI combined uncertainty from Table 4 and the uncertainty stated by the participant for the  $^{99m}\text{Tc}$ ,  $^{18}\text{F}$  and  $^{64}\text{Cu}$  measurements (see Table 2). The correlation between the POLATOM and the BIPM due to the use of the same  $^{99m}\text{Tc}$  and  $^{64}\text{Cu}$  half-life is negligible in view of the small contribution of these half-lives to the combined uncertainty of the measurements.

The K4 comparison results are given in Table 5a as well as the linked results  $A_e$  in the corresponding BIPM.RI(II)-K1 comparisons which were obtained by multiplying  $A_E$  by the linking factors given in Table 5b:

Table 5a: BIPM.RI(II)-K4. comparison results and link to the BIPM.RI(II)-K1 comparisons

Radionuclide	Measurement method ACRONYM*	Solution volume in the ampoules (calculated) /cm <sup>3</sup>	$A_E$ /kBq	$u(A_E)$ /kBq	Linked $A_e$ /kBq	$u(A_e)$ /kBq
$^{99m}\text{Tc}$	4 $\pi$ (LS)ce- $\gamma$ coincidence counting 4P-LS-CE-NA-GR-CO	3.63 and 3.63	12.710	0.092	154 600	1200
$^{18}\text{F}$	4 $\pi$ (LS) $\beta^+$ - $\gamma$ coincidence counting 4P-LS-PO-NA-GR-CO	3.63 and 3.62	10.249	0.058	15 323	88
$^{64}\text{Cu}$	4 $\pi$ (LS) $\beta^+$ - $\gamma$ coincidence counting 4P-LS-MX-NA-GR-CO	3.61 and 3.60	55.04	0.31	81 580	480

\* See appendix 1

Table 5b: Linking factors of BIPM.RI(II)-K4 comparison to BIPM.RI(II)-K1 comparison

Radionuclide	Linking factor	Provider of solution for measurement of linking factor at the BIPM
$^{99m}\text{Tc}$	12 165(23)	LNE-LNHB (2007 and 2014), NPL (2008)
$^{18}\text{F}$	1495.1(18)	LNE-LNHB (2014), AAA* (2014)
$^{64}\text{Cu}$	1482.2(25)	NPL (2016), CNRS/CEMHTI (2015)

\* Advanced Accelerator Applications

## 7. Key comparison reference values and degrees of equivalence

### 7.1 KCRVs update

In May 2013 the CCRI(II) decided to calculate the key comparison reference value (KCRV) using the power-moderated weighted mean [24] rather than an unweighted mean, as had been the policy. This type of weighted mean is similar to a Mandel-Paule mean in that the NMIs' uncertainties may be increased until the reduced chi-squared value is one. In addition, it allows for a power smaller than two in the weighting factor. As proposed in [21],  $\alpha$  is taken as  $2 - 3/N$  where  $N$  is the number of results selected for the KCRV. Therefore, all SIR key comparison results can be selected for the key comparison reference value (KCRV) with the following provisions:

- a) only results for solutions standardized by primary techniques are accepted, with the exception of radioactive gas standards (for which results from transfer instrument measurements that are directly traceable to a primary measurement in the laboratory may be included);
- b) each NMI or other laboratory has only one result (normally the most recent result or the mean if more than one ampoule is submitted);
- c) results more than 20 years old are included in the calculation of the KCRV (but are not included in data shown in the KCDB or in the plots in this report as they have expired);
- d) possible outliers can be identified on a mathematical basis and excluded from the KCRV using the normalized error test with a test value of 2.5 and using the modified uncertainties;
- e) results can also be excluded for technical reasons; and
- f) the CCRI(II) is always the final arbiter regarding excluding any data from the calculation of the KCRV.

All the submissions to the SIR since its inception in 1976 are maintained in a database known as the "master-file". The data set used for the evaluation of the KCRVs is known as the "KCRV file" and is a reduced data set from the SIR master-file.

Although the KCRV may be modified when other NMIs participate, on the advice of the Key Comparison Working Group of the CCRI(II), such modifications are made only by the CCRI(II) during one of its biennial meetings, or by consensus through electronic means (e.g., email) as discussed at the CCRI(II) meeting in 2013. In March 2015 and June 2017, the CCRI agreed for  $^{99m}\text{Tc}$  and  $^{18}\text{F}$ , respectively, that SIRTI linked results based on primary measurements or pressurized ionization chamber (IC) measurement are eligible for inclusion in the KCRV of the corresponding BIPM.RI(II)-K1 comparison when the IC is calibrated by a primary measurement of the same radionuclide within one year prior to the comparison date. In 2017, the CCRI also agreed that the limit of one year can be extended for practical reasons when the SIRTI comparison covers more than two nuclides at a time.

The  $^{99m}\text{Tc}$  SIR and SIRTI results previously included in the KCRV are given in Table 6a together with further SIRTI-eligible results. Using these results, the KCRV for  $^{99m}\text{Tc}$  calculated using the power moderated weighted mean is 153 090(380) kBq, with the power  $\alpha = 1.75$ . This can be compared successfully with the previous KCRVs of 153 070(460) kBq published in 2004 [28], 153 140(330) kBq published in 2005 [29], 153 240(220) kBq published in 2010 [27], 153 170(310) kBq published in 2016 [22], and with the value of 153 400(410) kBq obtained using the SIRIC [26] efficiency curves of the SIR.

**Table 6a:  $^{99m}\text{Tc}$  SIR and SIRTI linked results included in the calculation of the KCRV**

NMI	Comparison and year of participation	Measurement method	Comparison result $A_e$ / kBq	Reference
IRA	SIR, 1984	IC* calibrated in 1984 by $4\pi(\text{PC})e_c\text{-}\gamma$ coincidence, HPGe detector** and $4\pi(\text{NaI})\gamma$ counting	153 770(660)	[22]
PTB	SIR, 2005	IC calibrated in Nov. 2005 by $4\pi(\text{PC})e_c\text{-}x$ and $4\pi(\text{PPC})e_c\text{-}$ photon coincidences	152 710(640)	[22]
NPL	SIR, 2005	$4\pi(\text{PC})e_c\text{-}\gamma$ coincidence	153 310(660)	[22]
LNE-LNHB	SIR, 2007	$4\pi(\text{PC})\beta\text{-}\gamma$ anti-coincidence	153 180(790)	[22]
NIST	SIRTI, 2009	IC calibrated by anticoincidence measurements 2 months prior the comparison	152 840(730)	[22]
KRISS	SIRTI, 2010	IC calibrated by $4\pi(\text{LS})\beta\text{-}\gamma$ coincidence measurements 3 months prior the comparison	154 100(1400)	[22]
NIM	SIRTI, 2012	IC calibrated by coincidence measurements 4 months prior the comparison	153 100(1200)	[22]
LNMRI/IRD	SIRTI, 2013	IC calibrated by $4\pi(\text{LS})\beta\text{-}\gamma$ anticoincidence meas. 1 month prior the comparison	154 700(1700)	[22]
IFIN-HH	SIRTI, 2013	coincidence	150 400(1800)	[22]
ENEA-INMRI	SIRTI, 2014	$4\pi(\text{LS})e_c\text{-}\gamma(\text{NaI})$ coincidence	150 750(770)	[22]
NMISA	SIRTI, 2015	IC calibrated by $4\pi(\text{LS})\beta\text{-}\gamma$ coincidence measurements 2 months prior the comparison	156 100(2200)	[21]
POLATOM	SIRTI, 2016	$4\pi(\text{LS})e_c\text{-}\gamma$ coincidence	154 600(1200)	Present publication

\* pressurized ionization chamber (IC) with correction factor for self-absorption in the solution of 1.0037(10)

\*\* calibrated using  $^{57}\text{Co}$  and  $^{139}\text{Ce}$  calibrated sources

The  $^{18}\text{F}$  SIR results previously included in the KCRV are given in Table 6b together with the SIRTI eligible results. This is the first time that linked results from BIPM.RI(II)-K4.F-18 are included in the KCRV. The NPL has a result in both the K1 and K4 comparisons with similar relative uncertainty for the primary measurements (about 0.25 %). It was decided to use the K1 result in the KCRV as it has a smaller uncertainty contribution from the comparison itself (7

parts in 10 000 for the K1 and 19 parts in 10 000 for the K4 including the link uncertainty). Using these results, the KCRV for  $^{18}\text{F}$  calculated using the power moderated weighted mean is 15 293(19) kBq, with the power  $\alpha = 1.7$ . This can be compared with previous KCRVs of 15 241(71) kBq and 15 254(43) kBq published in 2003 [18, 19], 15 245(32) kBq in 2004 [16], 15 259(29) kBq in 2006 [25] and 15 276(24) kBq published in 2016 [14].

The KCRV for  $^{64}\text{Cu}$  has been defined in the frame of the BIPM.RI(II)-K1.Cu-64 comparison using direct contributions to the SIR, and is equal to 80 990(340) kBq [23].

**Table 6b:  $^{18}\text{F}$  SIR and SIRTI linked results included in the calculation of the KCRV**

NMI	Comparison and year of participation	Measurement method	Comparison result $A_e$ / kBq	Reference
IRA	SIR, 2001	IC calibrated by $4\pi\gamma(\text{NaI})$ counting and liquid scintillation	15 312(57)	[14]
NPL	SIR, 2003	$4\pi(\text{PC})\beta^+-\gamma$ coincidence method	15 281(39)	[14]
CIEMAT	SIR, 2004	IC calibrated by $4\pi\beta^+(\text{PPC})-\gamma$ coincidence	15 216(97)	[14]
PTB	SIR, 2005	IC calibrated by $4\pi\beta^+(\text{PC})-\gamma$ coincidence and CIEMAT/NIST	15 316(50)	[14]
LNE-LNHB	SIR, 2010	Liquid scintillation counting using TDCR	15 203(62)	[14]
VNIIM	SIRTI, 2014	$4\pi\gamma(\text{NaI})$ counting	15 197(97)	[20]
ENEA-INMRI	SIRTI, 2014	$4\pi(\text{LS})\beta^+-\gamma$ coincidence method, $4\pi\gamma(\text{NaI})$ counting, and TDCR	15 368(49)	[20]
NMISA	SIRTI, 2015	IC calibrated by $4\pi(\text{LS})\beta^+-\gamma$ coincidence method 1 month prior the comparison	15 328(96)	[21]
NIST	SIRTI, 2016	IC calibrated by $4\pi(\text{LS})\beta^+-\gamma$ anticoincidence method 9 month prior the comparison	15 291(64)	[15]
POLATOM	SIRTI, 2016	$4\pi(\text{LS})\text{ce}-\gamma$ coincidence	15 323(88)	Present publication

## 7.2 Degrees of equivalence

Every participant in a key comparison is entitled to have one result included in the key comparison database (KCDB) as long as the laboratory is a signatory or designated institute

listed in the CIPM MRA. Normally, the most recent result is the one included. Any participant may withdraw its result only if all the participants agree.

The degree of equivalence of a particular NMI,  $i$ , with the KCRV is expressed as the difference  $D_i$  with respect to the KCRV

$$D_i = A_{ei} - \text{KCRV} \quad (1)$$

and the expanded uncertainty ( $k = 2$ ) of this difference,  $U_i$ , known as the equivalence uncertainty, hence

$$U_i = 2u(D_i), \quad (2)$$

taking correlations into account as appropriate [24].

The degree of equivalence between any pair of NMIs,  $i$  and  $j$ , is expressed as the difference  $D_{ij}$  in their results

$$D_{ij} = D_i - D_j = A_{ei} - A_{ej} \quad (3)$$

and the expanded uncertainty of this difference  $U_{ij}$  where

$$U_{ij}^2 = 4u^2(D_{ij}) = 4[u_i^2 + u_j^2 - 2u(A_{ei}, A_{ej})] \quad (4)$$

where any obvious correlations between the NMIs (such as a traceable calibration) are subtracted using the covariance  $u(A_{ei}, A_{ej})$ , as is the correlation coming from the link of the SIRTI to the SIR. The covariance between two participants in the K4 comparison is given by

$$u(A_{ei}, A_{ej}) = A_{ei} A_{ej} (u_L/L)^2 \quad (5)$$

where  $u_L$  is the standard uncertainty of the linking factor  $L$  given above. However, the CCRI decided in 2011 that these pair-wise degrees of equivalence no longer need to be published as long as the methodology is explained.

Tables 7(a,b,c) show the matrices of the degrees of equivalence with the KCRV as they will appear in the KCDB. It should be noted that for consistency within the KCDB, a simplified level of nomenclature is used with  $A_{ei}$  replaced by  $x_i$ . The introductory text is that agreed for the comparison. The graph of the degrees of equivalence with respect to the KCRV (identified as  $x_R$  in the KCDB) is shown in Figure 4(a,b,c) in relative terms. The graphical representation indicates in part the degree of equivalence between the NMIs but obviously does not take into account the correlations between the different NMIs.

The CCRI(II)-K3.F-18 and APMP.RI(II)-K3.F-18 key comparisons have been linked to the BIPM.RI(II)-K1.F-18 key comparison earlier [17]. The degrees of equivalence have been updated following the update of the KCRV for  $^{18}\text{F}$  given above.

The degrees of equivalence of the BIPM.RI(II)-K1 key comparisons for  $^{99\text{m}}\text{Tc}$  and  $^{18}\text{F}$  have also been updated following the update of the KCRV for  $^{99\text{m}}\text{Tc}$  and  $^{18}\text{F}$ .

## Conclusion

In 2016, the POLATOM (Poland) hosted the SIRTI to participate in the BIPM ongoing key comparison for activity measurement of  $^{99m}\text{Tc}$ ,  $^{18}\text{F}$  and  $^{64}\text{Cu}$  (the BIPM.RI(II)-K4 series). These K4 comparisons are linked to the corresponding BIPM.RI(II)-K1 comparisons (the SIR comparisons).

The key comparison reference values for  $^{99m}\text{Tc}$  and  $^{18}\text{F}$ , usually defined in the frame of the K1 comparisons, have been updated to include recent results from the K4 comparisons, including from the POLATOM. This is the first time that  $^{18}\text{F}$  SIRTI results are included in the KCRV. The degrees of equivalence with the respective key comparison reference values have been evaluated for POLATOM's participation in the BIPM.RI(II)-K4 comparisons, and degrees of equivalence for other K1 or K4 participants and for the CCRI(II)-K3.F-18 and APMP.RI(II)-K3.F-18 key comparisons have been updated. The degrees of equivalence have been approved by the CCRI(II) and are published in the BIPM key comparison database.

Other results may be added when other NMIs contribute with  $^{99m}\text{Tc}$ ,  $^{18}\text{F}$  and  $^{64}\text{Cu}$  activity measurements to the K4 or K1 comparisons or take part in other linked Regional Metrology Organization comparisons. It should be noted that the final data in this paper, while correct at the time of publication, will become out-of-date as NMIs make new comparisons. The formal results under the CIPM MRA [7] are those available in the KCDB.



**Table 7a. Table of degrees of equivalence and introductory text for  $^{99m}\text{Tc}$**

**Key comparison BIPM.RI(II)-K1.Tc-99m**

**MEASURAND :** Equivalent activity of  $^{99m}\text{Tc}$

**Key comparison reference value: the SIR reference value for this radionuclide is  $x_R = 153.09 \text{ MBq}$  with a standard uncertainty,  $u_R = 0.38 \text{ MBq}$  (see Final Report).**

**The value  $x_i$  is the equivalent activity for laboratory  $i$ .**

The degree of equivalence of each laboratory with respect to the reference value is given by a pair of terms:

$D_i = (x_i - x_R)$  and  $U_i$ , its expanded uncertainty ( $k = 2$ ), both expressed in MBq, and

$U_i = 2((1 - 2w_i)u_i^2 + u_R^2)^{1/2}$  where  $w_i$  is the weight of laboratory  $i$  contributing to the calculation of  $x_R$ .

**Linking BIPM.RI(II)-K4.Tc-99m to BIPM.RI(II)-K1.Tc-99m**

**The value  $x_i$  is the SIRTI equivalent activity for laboratory  $i$  participant in BIPM.RI(II)-K4.Tc-99m having been normalized using the NPL and the LNE-LNHB as linking laboratories (see Final report).**

The degree of equivalence of laboratory  $i$  participant in BIPM.RI(II)-K4.Tc-99m with respect to the key comparison reference value is given

by a pair of terms:  $D_i = (x_i - x_R)$  and  $U_i$ , its expanded uncertainty ( $k = 2$ ), both expressed in MBq,

$U_i = 2((1 - 2w_i)u_i^2 + u_R^2)^{1/2}$  where  $w_i$  is the weight of laboratory  $i$  contributing to the calculation of  $x_R$ .

These statements make it possible to extend the BIPM.RI(II)-K1.Tc-99m matrices of equivalence to the other participants in BIPM.RI(II)-K4.Tc-99m.

**Table 7a continued**

Lab *i* ↓

	$D_i$	$U_i$
	/ MBq	
BEV	2.6	2.7
MKEH	1.3	3.3
PTB	-0.4	1.3
LNE-LNHB	0.1	1.6
NPL	0.2	1.7
NIST	-0.3	1.5
KRISS	1.0	2.7
NMIJ	-0.7	2.3
NIM	0.0	2.4
CNEA	7.1	4.3
LNMRI/IRD	1.6	3.3
IFIN-HH	-2.2	2.9
VNIIM	3.5	4.9
ENE-INMRI	-2.3	1.6
NMISA	3.0	4.3
POLATOM	1.5	2.4

**Figure 4a. Graph of degrees of equivalence with the KCRV for  $^{99m}\text{Tc}$**   
(as it appears in Appendix B of the MRA)

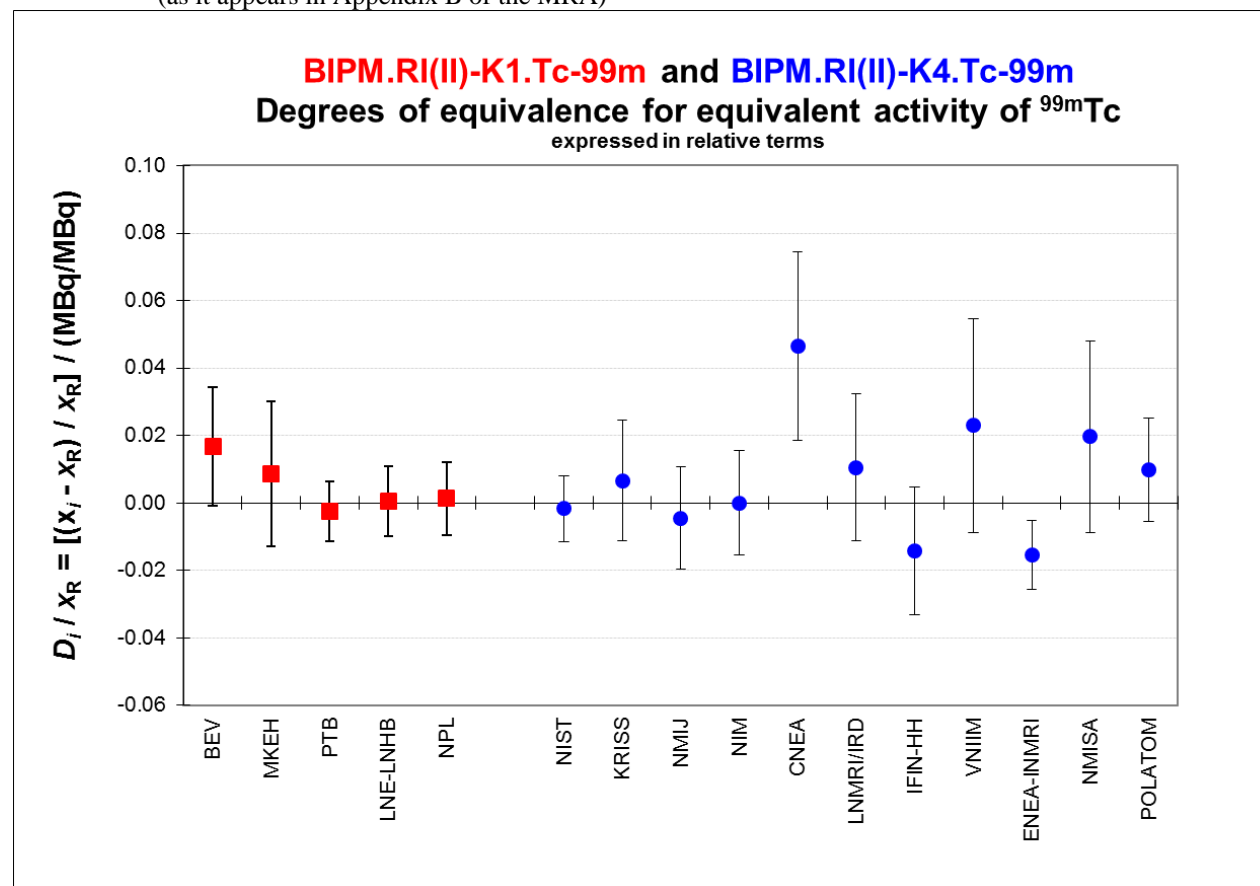




Table 7b continued

Linking APMP.RI(II)-K3.F-18 to BIPM.RI(II)-K1.F-18

The value  $x_i$  is the equivalent activity for laboratory  $i$  participant in APMP.RI(II)-K3.F-18 having been normalized using the NPL and the LNE-LNHB as linking laboratories (see [17]).

The degree of equivalence of laboratory  $i$  participant in APMP.RI(II)-K3. with respect to the key comparison reference value is given by a pair of terms:  $D_i = (x_i - x_R)$  and  $U_i$ , its expanded uncertainty ( $k = 2$ ), both expressed in MBq.

The approximation  $U_i = 2(u_i^2 + u_R^2)^{1/2}$  is used in the following table as this laboratory did not contribute to the KCRV.

These statements make it possible to extend the BIPM.RI(II)-K1.F-18 matrices of equivalence to all participants in the CCRI(II)-K3.F-18, the APMP.RI(II)-K3.F-18 and the BIPM.RI(II)-K4.F-18 comparisons.

Lab  $i$

	$D_i$ $U_i$	
	/ MBq	
IRA	0.02	0.11
BEV	0.10	0.32
CIEMAT	-0.08	0.19
PTB	0.023	0.093
LNE-LNHB	-0.09	0.12

VNIIM	-0.10	0.19
NPL	0.02	0.11
ENEA-INMRI	0.075	0.091
NMISA	0.03	0.19
NIST	0.00	0.12
POLATOM	0.03	0.17

ANSTO	-0.14	0.48
CMI-IIR	-0.28	0.24

INER	-0.16	0.30
------	-------	------

**Figure 4b. Graph of degrees of equivalence with the KCRV for  $^{18}\text{F}$**   
(as it appears in Appendix B of the MRA)

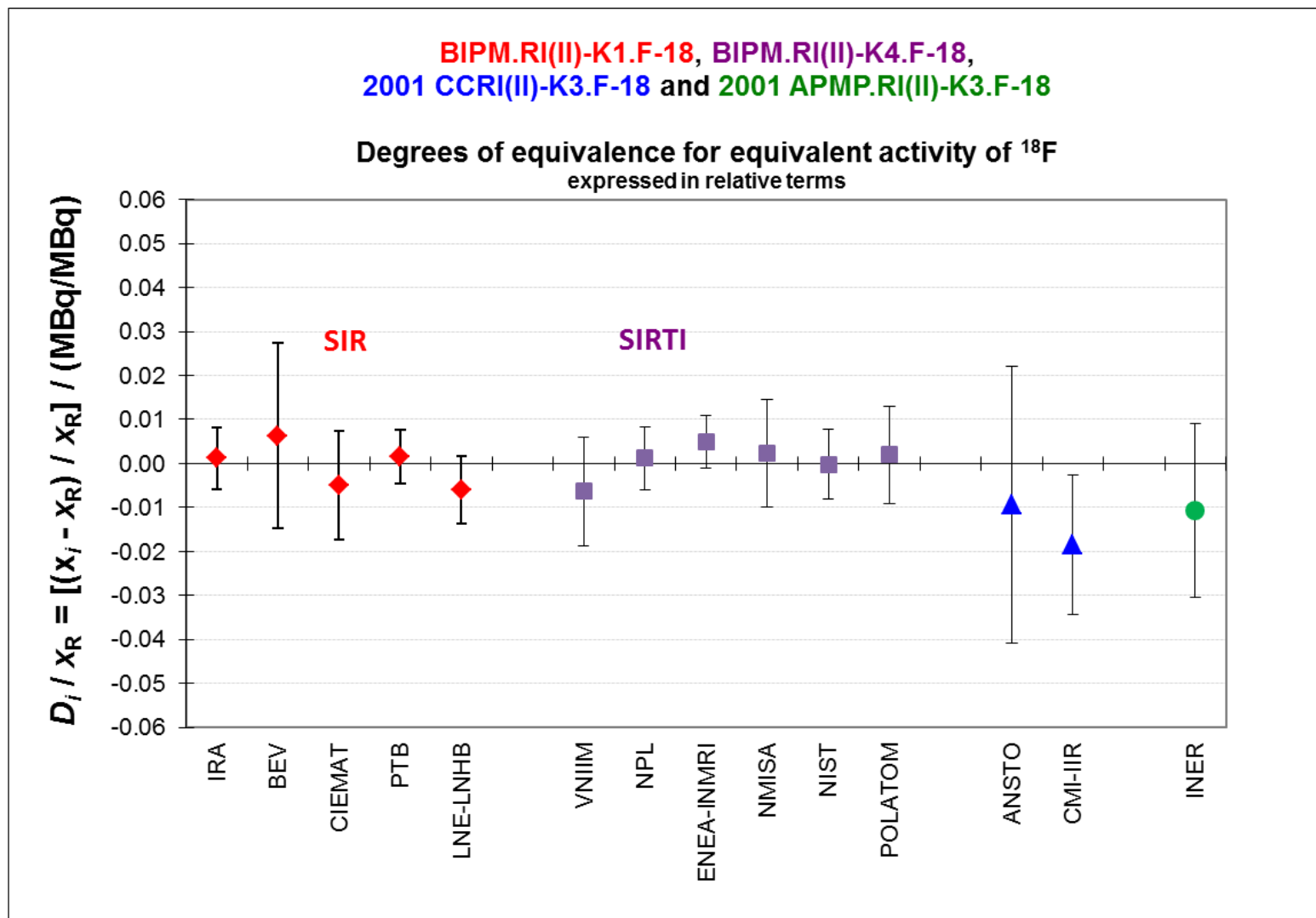


**Table 7c. Table of degrees of equivalence and introductory text for <sup>64</sup>Cu  
Key comparison BIPM.RI(II)-K1.Cu-64**

**MEASURAND :**                   Equivalent activity of <sup>64</sup>Cu

**Key comparison reference value: the SIR reference value  $x_R$  for this radionuclide is 80.99 MBq, with a standard uncertainty  $u_R$  of 0.34 MBq.**

**The value  $x_i$  is taken as the equivalent activity for laboratory  $i$ .**

The degree of equivalence of each laboratory with respect to the reference value is given by a pair of terms:

$D_i = (x_i - x_R)$  and  $U_i$ , its expanded uncertainty ( $k = 2$ ), both expressed in MBq, and

$U_i = 2((1 - 2w_i)u_i^2 + u_R^2)^{1/2}$  when each laboratory has contributed to the calculation of  $x_R$ .

Linking BIPM.RI(II)-K4.Cu-64 to BIPM.RI(II)-K1.Cu-64

**The value  $x_i$  is the SIRTI equivalent activity for laboratory  $i$  participant in BIPM.RI(II)-K4.Cu-64 multiplied by the linking factor to BIPM.RI(II)-K1.Cu-64 (see Final Report).**

The degree of equivalence of laboratory  $i$  participant in BIPM.RI(II)-K4.Cu-64 with respect to the key comparison reference value is given by a pair of terms:  $D_i = (x_i - x_R)$  and  $U_i$ , its expanded uncertainty ( $k = 2$ ), both expressed in MBq.

The approximation  $U_i = 2(u_i^2 + u_R^2)^{1/2}$  is used in the following table.

These statements make it possible to extend the BIPM.RI(II)-K1.Cu-64 matrices of equivalence to all participants in the BIPM.RI(II)-K4.Cu-64 comparisons.

Lab  $i$

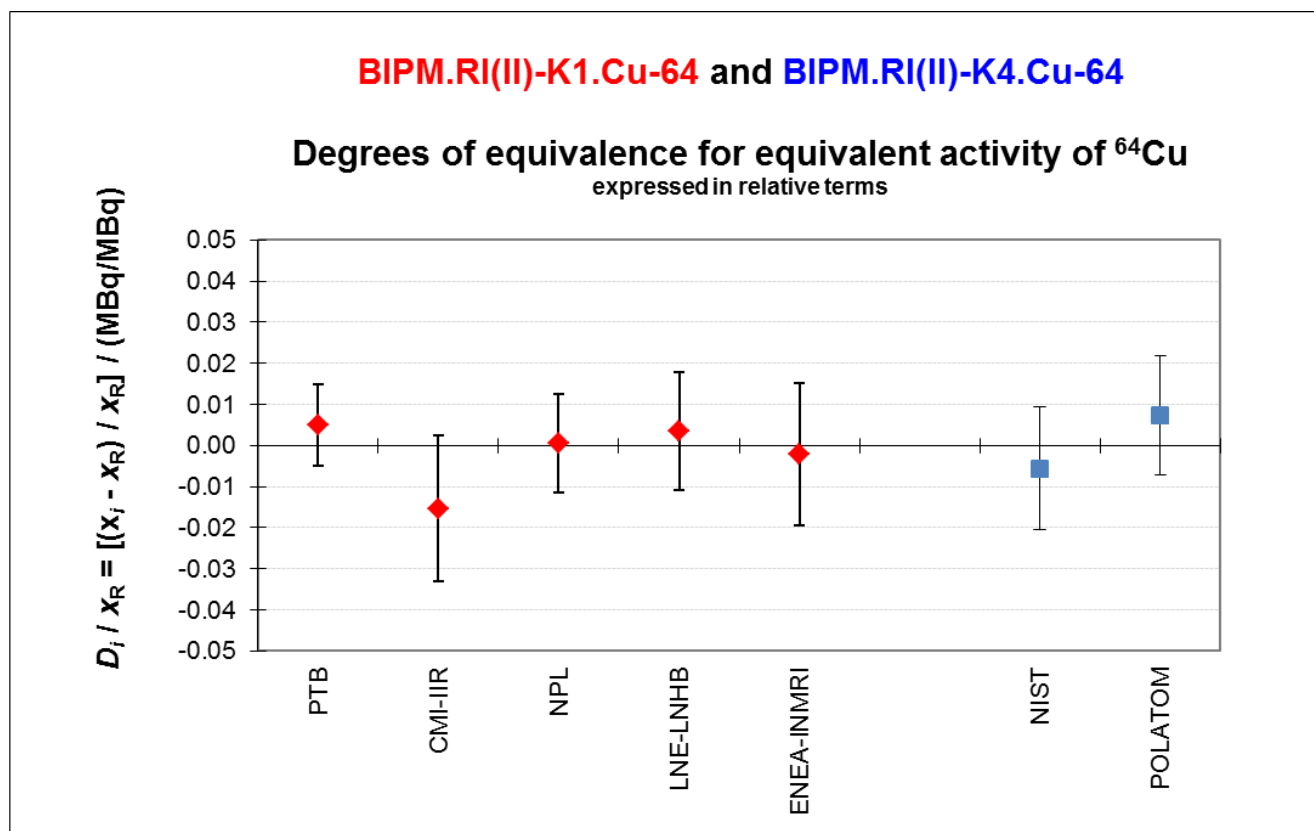


	$D_i$	$U_i$
	/ MBq	
PTB	0.41	0.80
CMI-IIR	-1.2	1.4
NPL	0.0	1.0
LNE-LNHB	0.3	1.2
ENEA-INMRI	-0.2	1.4

Table 7c continued

	$D_i$	$U_i$
	/ MBq	
NIST	-0.4	1.2
POLATOM	0.6	1.2

Figure 4c. Graph of degrees of equivalence with the KCRV for  $^{64}\text{Cu}$   
(as it appears in Appendix B of the MRA)



## References

- [1] Ratel G., 2007, The Système International de Référence and its application in key comparisons, *Metrologia* **44**(4), [S7-S16](#).
- [2] Remit of the CCRI(II) Transfer Instrument Working Group, 2009, CCRI(II) working document CCRI(II)/09-15.
- [3] Bé M.-M., Chisté V., Dulieu C., Browne E., Chechev V., Kuzmenko N., Helmer R., Nichols A., Schönfeld E., Dersch R., 2004, Table of radionuclides, *Monographie BIPM-5*, volume 1.
- [4] Bé M.-M., Helmer R., 2011, Decay Data Evaluation Project working group, [www.nucleide.org/DDEP\\_WG/DDEPdata.htm](http://www.nucleide.org/DDEP_WG/DDEPdata.htm).
- [5] NUDAT2.5, [National Nuclear Data Center](#), Brookhaven National Laboratory, based on ENSDF and the Nuclear Wallet Cards.
- [6] Bouchard J., 2000, *Appl. Radiat. Isot.* **52**, 441-446.
- [7] SIR Transfer Instrument. Protocol for the ongoing comparisons on site at the NMIs, BIPM.RI(II)-K4. Published on the [CIPM MRA KCDB website](#).
- [8] CIPM MRA: *Mutual recognition of national measurement standards and of calibration and measurement certificates issued by national metrology institutes*, International Committee for Weights and Measures, 1999, 45 pp. <http://www.bipm.org/pdf/mra.pdf>.
- [9] Michotte C. *et al.*, The SIRTI, a new tool developed at the BIPM for comparing activity measurements of short-lived radionuclides world-wide, *Rapport BIPM-2013/02*.
- [10] Michotte C. *et al.*, Calibration of the SIRTI against the SIR and trial comparison of  $^{18}\text{F}$  and  $^{99\text{m}}\text{Tc}$  at the NPL. *In preparation*.
- [11] Baerg A.P. *et al.*, 1976, Live-timed anti-coincidence counting with extending dead-time circuitry, *Metrologia* **12**, 77-80.
- [12] Fitzgerald R., 2016, Corrections for the combined effects of decay and dead time in live-timed counting of short-lived radionuclides, *Appl. Radiat. Isot.* **109**, 335-340.
- [13] Sibbens G., 1991, A comparison of NIST/SIR-, NPL-, and CBNM 5 ml ampoules, GE/R/RN/14/91, CEC-JRC Central Bureau for Nuclear Measurements, Belgium.
- [14] Michotte C. *et al.*, 2016, Update of the BIPM comparison BIPM.RI(II)-K1.F-18 of activity measurements of the radionuclide  $^{18}\text{F}$  to include the 2010 result of the LNE-LNHB (France). *Metrologia*, 2016, **53**, *Tech. Suppl.*, 06004.
- [15] Michotte C., Nonis M., Bergeron D., Cessna J., Fitzgerald R., Pibida L., Zimmerman B., Fenwick A., Ferreira K., Keightley J., Da Silva I., Activity measurements of the radionuclides  $^{18}\text{F}$  and  $^{64}\text{Cu}$  for the NIST, USA, in the ongoing comparisons BIPM.RI(II)-K4.F-18 and BIPM.RI(II)-K4.Cu-64, *Metrologia*, 2017, **54**, *Tech. Suppl.* 06011.
- [16] Ratel G., Michotte C., García-Toraño E., Los Arcos J.-M., Update of the BIPM comparison BIPM.RI(II)-K1.F-18 of activity measurements of the radionuclide  $^{18}\text{F}$  to include the CIEMAT, *Metrologia*, 2004, **41**, *Tech. Suppl.*, 06016.
- [17] Ratel G., Michotte C., Woods M.J., Comparisons CCRI(II)-K3.F-18 and APMP.RI(II)-K3.F-18 of activity measurements of the radionuclide  $^{18}\text{F}$  and links to the key comparison reference value of the BIPM.RI(II)-K1.F-18 comparison, *Metrologia*, 2005, **42**, *Tech. Suppl.*, 06007.
- [18] Ratel G., Michotte C., BIPM comparison BIPM.RI(II)-K1.F-18 of activity measurements of the radionuclide  $^{18}\text{F}$ , *Metrologia*, 2003, **40**, *Tech. Suppl.*, 06005.
- [19] Ratel G., Michotte C., Woods M.J., Update of the BIPM comparison BIPM.RI(II)-K1.F-18 of activity measurements of the radionuclide  $^{18}\text{F}$  to include the NPL, *Metrologia*, 2003, **40**, *Tech. Suppl.*, 06027.
- [20] Michotte C., Nonis M., Alekseev I.V., Kharitonov I.A., Tereshchenko E.E., Zanevskiy A.V., Keightley J.D., Fenwick A., Ferreira K., Johansson L., Capogni M., Carconi P.,



- Fazio A., De Felice P., Comparison of  $^{18}\text{F}$  activity measurements at the VNIIM, NPL and the ENEA-INMRI using the SIRTI of the BIPM, *Applied Radiation and Isotopes*, 2016, **109**, 17–23.
- [21] Michotte C., Nonis M., Van Rooy M.W., Van Staden M.J. and Lubbe J., Activity measurements of the radionuclides  $^{18}\text{F}$  and  $^{99\text{m}}\text{Tc}$  for the NMISA, South Africa in the ongoing comparisons BIPM.RI(II)-K4.F-18 and BIPM.RI(II)-K4.Tc-99m, *Metrologia*, 2017, **54**, *Tech. Suppl.*, 06001.
- [22] Michotte C., Nonis M., Alekseev I.V., Kharitonov I.A., Tereshchenko E.E., Zanevskiy A.V., Capogni M., De Felice P., Fazio A., Carconi P., Activity measurements of the radionuclide  $^{99\text{m}}\text{Tc}$  for the VNIIM, Russian Federation and ENEA-INMRI, Italy, in the ongoing comparison BIPM.RI(II)-K4.Tc-99m and KCRV update in the BIPM.RI(II)-K1.Tc-99m comparison, *Metrologia*, 2016, **53**, *Tech. Suppl.*, 06014.
- [23] Michotte C., *et al.*, Update of the BIPM comparison BIPM.RI(II)-K1.Cu-64 of activity measurements of the radionuclide  $^{64}\text{Cu}$  to include the 2009 results of the CMI–IIR (Czech Rep.) and the NPL (UK), the 2010 result of the LNE–LNHB (France) and the 2011 result of the ENEA–INMRI (Italy). *Metrologia*, 2013, **50**, *Tech. Suppl.*, 06021.
- [24] Pommé S., Keightley, J., Determination of a reference value and its uncertainty through a power-moderated mean, *Metrologia*, 2015, **52(3)**, S200-S212.
- [25] Ratel G., Michotte C., Kossert K., Janßen H., Update of the BIPM comparison BIPM.RI(II)-K1.F-18 of activity measurements of the radionuclide  $^{18}\text{F}$  to include the PTB, *Metrologia*, 2006, **43**, *Tech. Suppl.*, 06001.
- [26] Cox M.G., Michotte C., Pearce A.K., Measurement modelling of the International Reference System (SIR) for gamma-emitting radionuclides, Monographie BIPM-7, 2007, 48 pp.
- [27] Michotte C., Courte S., Ratel G., Moune M., Johansson L., Keightley J., Update of the BIPM.RI(II)-K1.Tc-99m comparison of activity measurements for the radionuclide  $^{99\text{m}}\text{Tc}$  to include new results for the LNE-LNHB and the NPL, *Metrologia*, 2010, **47**, *Tech. Suppl.*, 06026.
- [28] Ratel G., Michotte C., BIPM comparison BIPM.RI(II)-K1.Tc-99m of activity measurements of the radionuclide  $^{99\text{m}}\text{Tc}$ , *Metrologia*, 2004, **41**, *Tech. Suppl.*, 06005.
- [29] Ratel G., Michotte C., Johansson L., Update of the BIPM.RI(II)-K1.Tc-99m comparison of activity measurements for the radionuclide  $^{99\text{m}}\text{Tc}$  to include the NPL, *Metrologia*, 2005, **42**, *Tech. Suppl.*, 06015.

**Appendix 1. Acronyms used to identify different measurement methods**

Each acronym has six components, geometry-detector (1)-radiation (1)-detector (2)-radiation (2)-mode. When a component is unknown, ?? is used and when it is not applicable 00 is used.

<b>Geometry</b>	<b>acronym</b>	<b>Detector</b>	<b>acronym</b>
4 $\pi$	4P	proportional counter	PC
defined solid angle	SA	press. prop. counter	PP
2 $\pi$	2P	liquid scintillation counting	LS
undefined solid angle	UA	Nal(Tl)	NA
		Ge(HP)	GH
		Si(Li)	SL
		CsI(Tl)	CS
		ionization chamber	IC
		grid ionization chamber	GC
		Cerenkov detector	CD
		calorimeter	CA
		solid plastic scintillator	SP
		PIPS detector	PS
		CeBr3	CB
<b>Radiation</b>	<b>acronym</b>	<b>Mode</b>	<b>acronym</b>
positron	PO	efficiency tracing	ET
beta particle	BP	internal gas counting	IG
Auger electron	AE	CIEMAT/NIST	CN
conversion electron	CE	sum counting	SC
mixed electrons	ME	coincidence	CO
bremsstrahlung	BS	anti-coincidence	AC
gamma rays	GR	coincidence counting with efficiency tracing	CT
X - rays	XR	anti-coincidence counting with efficiency tracing	AT
photons ( $x + \gamma$ )	PH	triple-to-double coincidence ratio counting	TD
alpha - particle	AP	selective sampling	SS
mixture of various radiations	MX	high efficiency	HE

**Examples**

<b>Method</b>	<b>acronym</b>
4 $\pi$ (PC) $\beta$ - $\gamma$ -coincidence counting	4P-PC-BP-NA-GR-CO
4 $\pi$ (PPC) $\beta$ - $\gamma$ -coincidence counting eff. trac.	4P-PP-MX-NA-GR-CT
defined solid angle $\alpha$ -particle counting with a PIPS detector	SA-PS-AP-00-00-00
4 $\pi$ (PPC)AX- $\gamma$ (Ge(HP))-anticoincidence counting	4P-PP-MX-GH-GR-AC
4 $\pi$ CsI- $\beta$ ,AX, $\gamma$ counting	4P-CS-MX-00-00-HE
calibrated IC	4P-IC-GR-00-00-00
internal gas counting	4P-PC-BP-00-00-IG